



**Study of corrosion inhibition of copper in synthetic seawater by *Equisetum arvense* as green corrosion inhibitor**

**Estudio de inhibición de la corrosión del cobre en agua de mar sintética por *Equisetum arvense* como inhibidor verde de la corrosión**

A. Esquivel-Rojas<sup>1</sup>, C. Cuevas-Arteaga<sup>1\*</sup>, M.G. Valladares-Cisneros<sup>2</sup>

<sup>1</sup>Instituto de Investigación en Ciencias Básicas y Aplicadas, Centro de Investigación en Ingeniería y Ciencias Aplicadas. Universidad Autónoma del Estado de Morelos. Av. Universidad 1001 Col. Chamilpa, Cuernavaca Morelos, C. P. 62209.

<sup>2</sup>Facultad de Ciencias Químicas e Ingeniería, Universidad Autónoma del Estado de Morelos, Av. Universidad 1001, Col. Chamilpa, Cuernavaca, Morelos, C.P. 62209.

Received: May 30, 2019; Accepted: September 20, 2019

**Abstract**

Extract of the stems of *Equisetum arvense* was studied as green corrosion inhibitor (GCI) in synthetic seawater exposing samples of copper. In order to determine the protection of the metal by the GCI, electrochemical tests were performed using potentiodynamic polarization curves (PPC), electrochemical impedance spectroscopy (EIS) and linear polarization resistance (LPR) at room temperature. The morphological characterization of the material with and without GCI was carried out by scanning electron microscopy (SEM). The chemical composition of the GCI was determined by Fourier transform-infrared spectroscopy (FTIR) and gas chromatography coupled to mass spectrometry (GC-MS). The results showed that *Equisetum arvense* acts as a mixed-type GCI, achieving an inhibition efficiency (IE) of 53.78% when using 1000 ppm of GCI from PPC. From EIS the charge transfer resistance increased in the first 21 h, obtaining an IE of 87.5%. LPR results showed similar behavior than EIS at the same concentration. FTIR revealed that the chemical structure of the compounds of methanol extract of *Equisetum arvense* have functional groups such as: -OH, C-H, C=O and C-O, whereas GC-MS showed that eight compounds are present in the GCI.

**Keywords:** Green corrosion inhibitor, *Equisetum arvense*, copper, synthetic seawater.

**Resumen**

Se estudió el extracto de los tallos de *Equisetum arvense* como inhibidor verde de la corrosión (IVC) en muestras de cobre inmersas en agua de mar sintética. Para determinar el efecto de protección del IVC, se realizaron pruebas electroquímicas usando curvas de polarización potenciodinámica (CPP), espectroscopia de impedancia electroquímica (EIE) y resistencia a la polarización lineal (RPL) a temperatura ambiente. La caracterización morfológica del material con y sin IVC se realizó mediante microscopía electrónica de barrido (MEB). La composición química del IVC se determinó por medio de espectroscopia infrarroja por transformada de Fourier (FTIR) y cromatografía de gases acoplada a espectrometría de masas (CG-EM). Los resultados mostraron que *Equisetum arvense* actúa como un IVC de tipo mixto, logrando una eficiencia de inhibición (EI) de 53.78% cuando se usan 1000 ppm por CPP. A partir de la EIE, la resistencia de transferencia de carga aumentó en las primeras 21 h, obteniendo una EI del 87.5%. Los resultados de RPL mostraron un comportamiento similar a la EIE en la misma concentración. FTIR reveló que el extracto metanólico de *Equisetum arvense* está constituido por grupos funcionales como: -OH, C-H, C=O y C-O, mientras que CG-EM mostró que son ocho los compuestos presentes en el IVC.

**Palabras clave:** Inhibidor verde de la corrosión, *Equisetum arvense*, cobre, agua de mar sintética.

**1 Introduction**

Different types of metallic materials have been used to improve the quality of life of modern society and the industrial progress. The metallic materials

are mainly used in pipes, bridges, building structure and industries among others (Callister and Rethwisch, 2009). Over time the useful life of metal materials depends on the environmental conditions and the corrosion media.

\* Corresponding author. E-mail: ccuevas@uaem.mx

<https://doi.org/10.24275/rmiq/Mat629>

issn-e: 2395-8472

Table 1. Green corrosion inhibitors studied for inhibiting the corrosion of Copper.

Green corrosion inhibitors	Aggressive medium	Concentration of the corrosion inhibition	IE %*	Reference
<i>Chenopodium ambrosioides</i>	HNO <sub>3</sub>	250 ppm	89.9	Motawea, et al. (2019)
<i>Ziziphus lotus</i>	Natural seawater	5000 ppm	93	Oukhrib et al. (2017)
<i>Olea europaea</i>	0.5 M NaCl	2.42 mmol L <sup>-1</sup>	90	Rahal et al. (2016)
<i>Crocus sativus</i>	Natural seawater	2000 ppm	84	Oukhrib et al. (2015)
<i>Emblica officinalis</i>	Natural seawater	1000 ppm	88.09	Rani and Selvaraj (2010)
Natural honey	0.5 M NaCl	1000 ppm	89	El-Etre (1998)

\*IE %: Inhibition efficiency percent

The study of "corrosion costs and preventive strategies in the United States", carried out during the years from 1999 to 2001, estimated that the annual cost generated during the three years due to corrosion issues is \$276 billion dollars, corresponding to an investment of 3.1% of Gross Domestic Product (GDP) (Kosh et al., 2002). The costs of addressing the problems caused by corrosion are related to accidents, often with human losses, contamination of raw material or product leakage and the partial or total stoppage of production processes for one or more days, as well as the environmental damage caused by the pollution of air, soil and groundwater among others (Raichev et al., 2009).

There are different methods to reduce the corrosive attack on metallic materials, but one of the most utilized is the use of corrosion inhibitors, since they constitute one of the most economical and practical methods in the industrial installations (Singh et al., 2016; Al-Otaibi et al., 2014). The inhibitors retard the corrosion rate of metals, and they are added to the corrosive medium, reducing the reaction between the metal and the medium. The inhibitors react with the metal surface or the environment to which the surface is exposed, providing certain level of protection. Some inhibitors are adsorbed protecting the surface of the metal by the formation of a film (Sastri, 2001; Anupama et al., 2015). Various synthetic organic compounds have been studied as corrosion inhibitors with adequate inhibition efficiencies, unfortunately most of these compounds are toxic for living beings and the environment (Abdallah et al., 2010; Banerjee et al., 2012).

In response to the issue of environmental compatibility, it is still looking for environmental friendly alternatives, so that plants have become a suitable study option for the development of new natural and ecological inhibitors. Organic extracts from different plant species have been studied, which have been obtained from leaves, seeds, fruits, bark and/or roots; all these vegetal extracts have natural compounds such as tannins, alkaloids, flavonoids, terpenoids, and carbohydrates among others, showing to be efficient corrosion inhibitors of metallic materials at laboratory level (Oguzie 2008; Abdullah 2011; Li et al., 2012; Fares et al., 2012; Flores-De los Ríos et al., 2015).

Among some natural species that have been studied and reported as corrosion inhibitors for copper, it is possible to mention some of them in table 1. Such inhibitors have been studied in some diverse corrosive media at different concentrations, reporting the inhibition efficiencies, which are in an interval from 84 to 94 %.

*Equisetum arvense* (*E. arvense*), commonly known as horsetail, is a plant belonging to Equisetaceae family, and it has been mainly used in traditional medicine due to its diuretic and antioxidant properties, so it has been reported that the fitoextract of *E. arvense* could retard or inhibit the oxidizing-reducing processes produced during the metallic corrosion (Asgarpanah and Roohi, 2012; Pallag et al., 2016; Pallag et al., 2018). According to some studies carried out by Oniszczyk et al., 2014, the horsetail extract was analyzed by a high-performance liquid chromatography (HPLC) technique, determining the

next chemical compounds: caffeic acid, chlorogenic acid, ferulic acid, kaempferol, quercetin, isoquercetin, apigenin and luteolin (Al-Snafi, 2017). Because of the horsetail extract presents natural chemical compounds containing oxygen atoms and/or aromatic rings in their chemical structure, which could reduce the oxidative reaction rate, the present work is concerned to the study of the corrosion performance of copper exposed in synthetic seawater at room temperature through the use of *E. arvense* as inhibitor, applying several electrochemical techniques named potentiodynamic polarization curves (PPC), electrochemical impedance spectroscopy (EIS) and lineal polarization resistance (LPR). In the industry, the use of copper as a noble material is very important due to its good thermal and electrical conductivities and its outstanding mechanical properties, however, the copper may be susceptible to corrosion in seawater due to the presence of chloride ions.

## 2 Materials and methods

### 2.1 Natural inhibitor preparation

Stems of *E. arvense* were obtained from a supermarket in Cuernavaca Morelos-México. The stems were cut and dehydrated for two weeks outdoors at room temperature in darkness condition. Subsequently, the stems were subjected to a maceration process with methanol during 48 h. Afterwards, the solvent was filtered and eliminated by reducing the pressure distillation using a rotary evaporator. As a final product, a viscous extract was obtained, having a greenish coloration and a characteristic odor. This material was considered as “the green corrosion inhibitor (GCI)”. A high concentration of the GCI solution of 10000 ppm was prepared, which was used for making several dilutions in concentrations of 250 and 1000 ppm. These two solutions of different concentrations were used for the study of the corrosion inhibitory activity through an electrochemical cell of 50 ml.

### 2.2 Metallic material

A copper rod (99% Cu) of 0.5 in diameter was used. For the electrochemical tests, copper specimens of approximately 0.5 cm length were cut, to which a groove was made in order to connect a copper wire for the electrical contact. Then, the sample with electrical

contact was encapsulated in glass resin leaving an exposed surface of 1.13 cm<sup>2</sup>. The samples were ground to 600 grit silicon carbide paper, rinsed with distilled water, degreased with acetone and dried under a warm air stream.

### 2.3 Electrolytic solution

The synthetic seawater was prepared according to the standard ASTM D1141-98 (2003), whose composition in g/L is 24.53NaCl, 5.2MgCl, 4.09Na<sub>2</sub>SO<sub>4</sub>, 1.16CaCl, 0.695KCl, 0.201NaHCO<sub>3</sub>, 0.101KBr, 0.027H<sub>3</sub>BO<sub>3</sub>, 0.025SrCl<sub>2</sub>, 0.003NaF.

### 2.4 Corrosion measurements

The electrochemical cell was constituted by a conventional three-electrode arrangement. An Ag/AgCl reference electrode, a platinum wire as an auxiliary electrode and the working electrode. This electrochemical cell was used for all the electrochemical tests. The electrochemical measurements started after 40 min of exposing the specimen to the corrosive medium, and when the corrosion potential reached a stable condition. The PPC's were carried out in a potential range from -600 to 400 mV respect to the corrosion potential with a sweep rate of 60 mVmin<sup>-1</sup>. The corrosion parameters such as: corrosion potential ( $E_{corr}$ ), corrosion current density ( $i_{corr}$ ), anodic slope ( $\beta_a$ ) and cathodic slope ( $\beta_c$ ) were determined by the Tafel extrapolation method, whereas the inhibition efficiency percentage (IE %) was calculated from the Eq. (1).

$$IE \% = \frac{(i_{corr}^0 - i_{corr})}{i_{corr}^0} \times 100 \quad (1)$$

where  $i_{corr}^0$  and  $i_{corr}$  are the corrosion current densities without and with the inhibitor, respectively.

The Electrochemical impedance spectroscopy tests were performed in a frequency range of 30 KHz to 0.01 Hz with a sinusoidal wave of 10 mV, obtaining the measurements each three hours. The corrosion IE % was determined by the Eq. (2).

$$IE \% = \frac{R_{ct} - R_{ct}^0}{R_{ct}} \times 100 \quad (2)$$

where  $R_{ct}$  and  $R_{ct}^0$  are the charge transfer resistances with and without the inhibitor.

The linear polarization resistance was used to obtain the polarization resistance ( $R_p$ ). The  $R_p$  was also obtained each three hours. Measurements were

carried out at  $\pm 10$  mV. The corrosion current density was determined from the Eq. (3).

$$i_{corr} = \frac{\beta_a}{2.303 \cdot R_p} \quad (3)$$

where  $i_{corr}$  is the corrosion current density,  $R_p$  is the polarization resistance and  $\beta_a$  is the anodic slope. RPL and EIS techniques were performed in sequence using the same sample of copper during ten days. The morphological characterization of the corroded copper specimens used for the RPL and EIS techniques after ten days of immersion were performed by the SEM Leo VP microscope (variable pressure) 1450. In order to determine the type of corrosion products formed over the copper, EDS analyses were made, afterwards the corroded samples were cleaned from the corrosion products, and analyzed once again to determine the type of corrosion suffered by the copper.

### 2.5 Inhibitor characterization

In order to determine the chemical functional groups of the pure extract, an analysis was made through the Fourier transform-infrared spectroscopy (FTIR) technique using an infrared spectrophotometer Alpha Bruker with data processing software system OPUS 7.2. The analysis was performed by scanning the sample in a wavelength range from 400 to 4000  $\text{cm}^{-1}$ . The separation of the majority chemical components present in the GCI was carried out in a Gas Chromatography coupled to Mass Spectrometry (GC-MS) Agilent 6890 System Plus coupled to Agilent 5973 Network detector mass selective. The GC-MS is equipped with a 5% phenyl-methyl-Silicone capillary column 30 m long, 250  $\mu\text{m}$  diameter and a wall thickness of 0.25  $\mu\text{m}$ . The programming of the temperature ramp was:  $T_i$  45  $^\circ\text{C}$ ,  $T_f$  250  $^\circ\text{C}$  with a gradient of 10  $^\circ\text{C}/\text{min}$ . The fragmentation pattern of the separate compounds was compared to the database of the same equipment N-15598, Rev. D 02.00 Mass Spectral Libraries.

## 3 Results and discussion

### 3.1 Potentiodynamic polarization curves

The polarization curves for copper in synthetic seawater in absence and in the presence of the two different concentrations of the GCI are shown in Fig. 1. The Tafel extrapolation method was applied to the PPC, obtaining the corrosion potential ( $E_{corr}$ ), the corrosion current density ( $i_{corr}$ ) and the anodic slope ( $\beta_a$ ), which are shown in table 2. The PPC showed active-passive behavior. It can be observed that the addition of the GCI decreased the  $i_{corr}$ . The anodic branch of the PPC's presents a Tafel region close to the  $E_{corr}$ , which was due to the dissolution of copper. A decrease of  $i_{corr}$  from 21 to 1  $\text{mA}/\text{cm}^2$  was also seen, which was due to the formation of a CuCl film. The CuCl film was dissolved to a potential of 50 mV approximately, which was due to its poor adhesion to the metallic surface. This film is transformed into a  $\text{CuCl}_2^-$  soluble complex, which is responsible for the dissolution of copper causing an increase of the  $i_{corr}$  until a limit value observed in a potential interval from 300 to 900 mV (Hu *et al.*, 2001; Chen *et al.*, 2012). With the addition of the inhibitor, it can be observed the same behavior with a small displacement of the cathodic curves. In addition, there is a slight change of  $E_{corr}$  towards more positive values in the presence of the GCI, suggesting that the inhibitor mainly acts in the anodic reaction.

The values of  $E_{corr}$  oscillate between -184.36 and -208.73 mV. According to literature an inhibitor can be classified as anodic or cathodic inhibitor if the value of  $E_{corr}$  has a displacement greater than 85 mV compared to that of the corrosive solution without GCI, otherwise, it would be a mixed-type inhibitor (Shylesha *et al.*, 2011; Deyab *et al.*, 2015). In this study, the displacement was of 24 mV, so that, the GCI can be classified as a mixed-type inhibitor. Likewise,  $\beta_a$  does not have a significant shift with respect to that obtained from the corrosive solution without GCI.

Table 2. Electrochemical parameters of copper obtained from the PPC's in synthetic seawater without and with GCI *E. arvensis*.

GCI (ppm)	$i_{corr}$ ( $\text{mA}/\text{cm}^2$ )	$E_{corr}$ (mV)	$\beta_a$ (mV/dec)	IE %
0	0.007826	-208.73	-67.96	—
250	0.003733	-201.94	-59.51	52.3
1000	0.003617	-184.36	-36.05	53.78

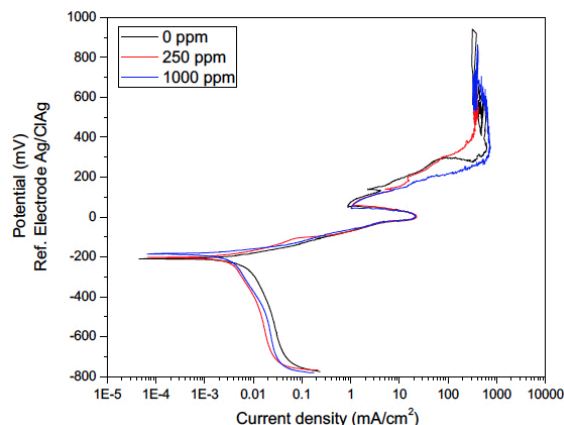


Fig. 1. Potentiodynamic polarization curves of copper in synthetic seawater using 0, 250 and 1000 ppm of *E. arvense* as GCI.

This fact suggests that the inhibitor was adsorbed on the surface of the copper, blocking the active sites of the metal without affecting the corrosion mechanism (Al-Mhyawi, 2014). On the other hand, the cathodic curve does not show a Tafel region, suggesting the influence of a mass transfer process in the corrosion mechanism.  $i_{corr}$  decreased from 0.007826 to 0.003617 mA/cm<sup>2</sup>, obtaining an IE of 52.30 and 53.78% for 250 and 1000 ppm respectively.

### 3.2 Electrochemical impedance spectroscopy

Nyquist diagrams of copper in synthetic seawater without and with GCI for ten days are shown in Fig. 2. The Nyquist diagrams show a depressed semicircle in the high frequency region. Some Nyquist diagrams showed a straight line in the low frequency values. The semicircle at high frequency is attributed to the charge transfer resistance, whereas the straight line at low frequency is attributed to the Warburg's impedance related to the species diffusion, either from the metallic surface to the bulk of the corrosive solution or from the bulk of the corrosive solution to the metallic surface (Pallag et al., 2016).

According to the observations in the Bode diagrams (angle and module) of copper exposed to synthetic seawater without and with GCI for ten days (Fig. 3), two time constants are seen. The time constant in the region of high frequency is related to the behavior of the corrosion products or film formed on the copper surface, whereas the time constant in the region of low frequencies is associated to the charge transfer reactions occurring in the pores and defects of the film, which determines the oxidation-

reduction processes (Feng et al., 2011; Tian et al., 2011; Hong et al., 2012). Only in the case of 1000 ppm there is a time constant around 144 h related to the charge transfer phenomenon. The formation of corrosion products results in an increase in the maximum phase angle, which indicates the inhibition of the corrosion process. Bode modulus diagrams of the blank and 250 ppm show that the impedance values increase in time when exposed in synthetic seawater until 216 h and then decreases. However, at 1000 ppm of GCI, the impedance decreases during the first 12 h and subsequently increases until 21 h, after that oscillations are seen.

The electrochemical parameters were determined from the equivalent circuits shown in Fig. 4, which have been suitable for the analysis of EIS data with a chi-squared value of magnitude  $10^{-4}$  for the blank and 250 ppm. For 1000 ppm the value of chi squared is in the order of magnitude of  $10^{-3}$  and  $10^{-4}$ . Where  $R_s$  represents the solution resistance,  $R_f$  the film resistance and  $R_{ct}$  the charge transfer resistance. The constant phase elements (CPE1 and CPE2) were used to represent the capacitance of film and the double layer capacitance respectively due to the non-homogeneous copper surface, whereas W is the Warburg impedance.

The equivalent circuits of Figs. 4a and 4b were used for the fitting from the beginning to 24 h respectively for the blank (without GCI); whereas the equivalent circuit showed in Fig. 4c was used for the results obtained from 48 h to the 240 h. For the study case with the addition of 250 ppm of GCI, the equivalent circuit of Fig. 4c was used. For the study case with the addition of 1000 ppm, the equivalent circuit of Fig. (4c) was used from the beginning to 144 h, and the equivalent circuit presented in Fig. (4d) was used for the rest of the exposure time.

The  $R_s$  values of the blank oscillate between 3 and 4  $\Omega \cdot \text{cm}^2$ , the  $R_s$  values for 250 ppm are around 2  $\Omega \cdot \text{cm}^2$  and between 7 to 5  $\Omega \cdot \text{cm}^2$  for 1000 ppm in the time. In the case of 1000 ppm, this variation may be due to the fact that during the first hours of exposure the ions and electrons from the oxidation-reduction reactions may reduce their interaction between the metal/solution interface due to the initially formed film on the surface of the copper. The subsequent interaction between both species could be easier due to the dissolution of such film (Gipi et al., 2009). The  $R_f$  values showed an increase for the blank, which can indicate the formation of corrosion products on the surface of the metal.

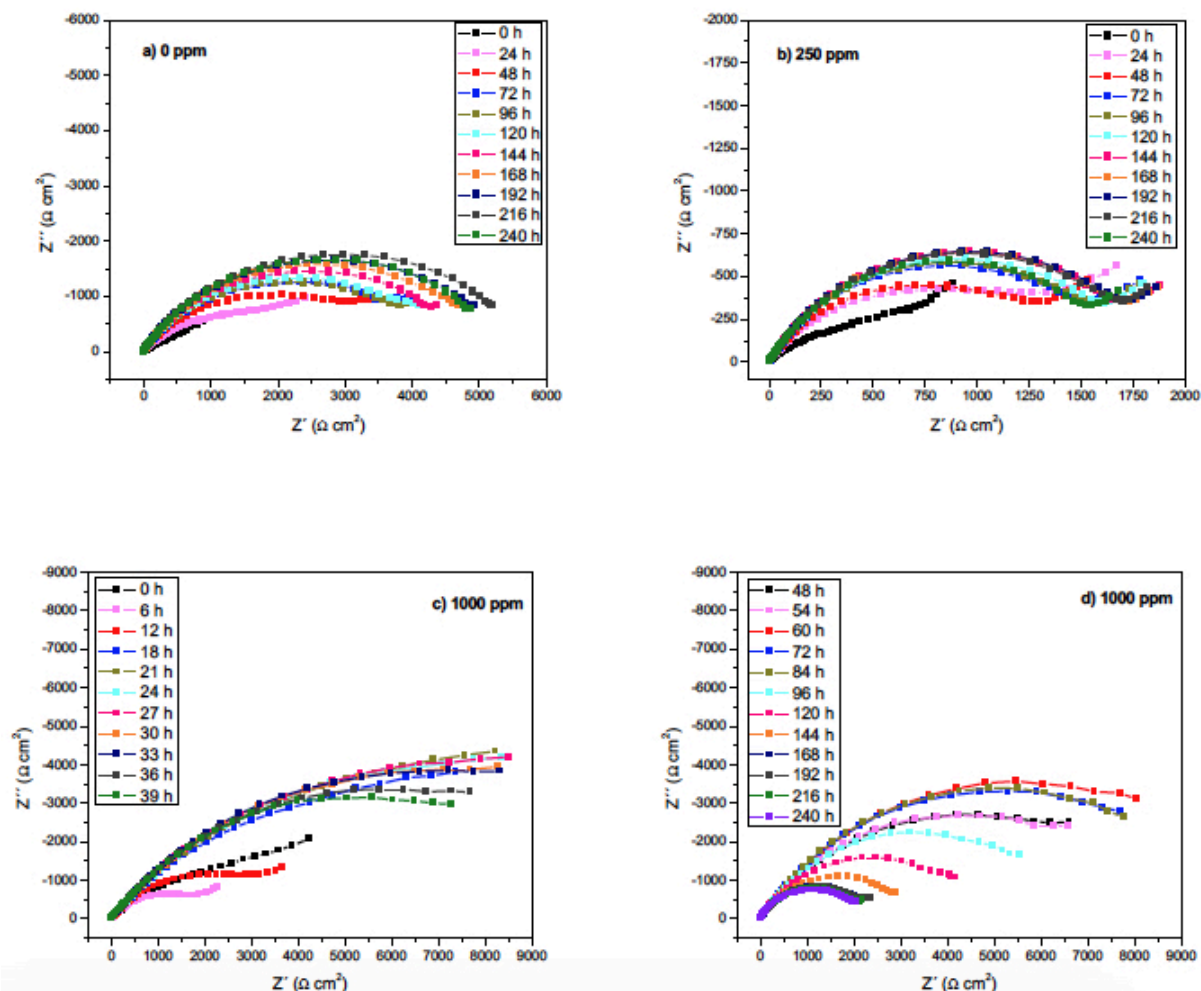


Fig. 2. Nyquist diagrams of copper exposed in synthetic seawater (a) without GCI, (b) with 250 ppm of GCI and (c, d) 1000 ppm of GCI *E. arvensis*.

Whereas at 250 ppm there is a non-significant increase (20 to 80  $\Omega \cdot \text{cm}^2$ ), keeping almost constant during the ten days of exposure, being these values lower than those obtained for copper without GCI. For 1000 ppm,  $R_f$  has a significant increase up to 84 h, afterward, a significant decrease was seen, which can be due to the dissolution of the film formed on the surface of copper. From 144 h there is only one-time constant, which means that there is only the charge transfer process. The behavior of  $R_{ct}$  showed in Fig. 5 is similar than that of  $R_f$  for the blank and 250 ppm. At 1000 ppm, it can be observed an increase in resistance up to 21 h, this increase can be attributed to the adsorption of the GCI on the electrode surface (Raj and Nallaiyan, 2012). After this time the  $R_{ct}$  decreased, but their values are major than that of the blank until 96 h.

The values of CPE-f of the blank suffer a decrease from 90 to 70  $\mu\text{F} \cdot \text{cm}^2$ , indicating the formation of corrosion products, whereas an increase from 47 to 175  $\mu\text{F} \cdot \text{cm}^2$  of the CPE-f at 250 ppm was observed. The CPE-f at 1000 ppm decreased until 27 h and subsequently increased until the end of the exposure. The results of CPE-ct is shown in Fig. 6, through which, it can be observed that CPE-ct values which, it can be observed that CPE-ct values decreased. For 1000 ppm there is a decrease until 144 h indicating the adsorption of the GCI on the surface of the metal, afterwards, the CPE-ct increases due to the possible dissolution of the adsorbed GCI over the metallic surface. According to Brunoro *et al.*, 2003, the increase of any CPE indicates that the formation of the film over the metallic surface is improbable or in case of its formation, the film can present more defects.

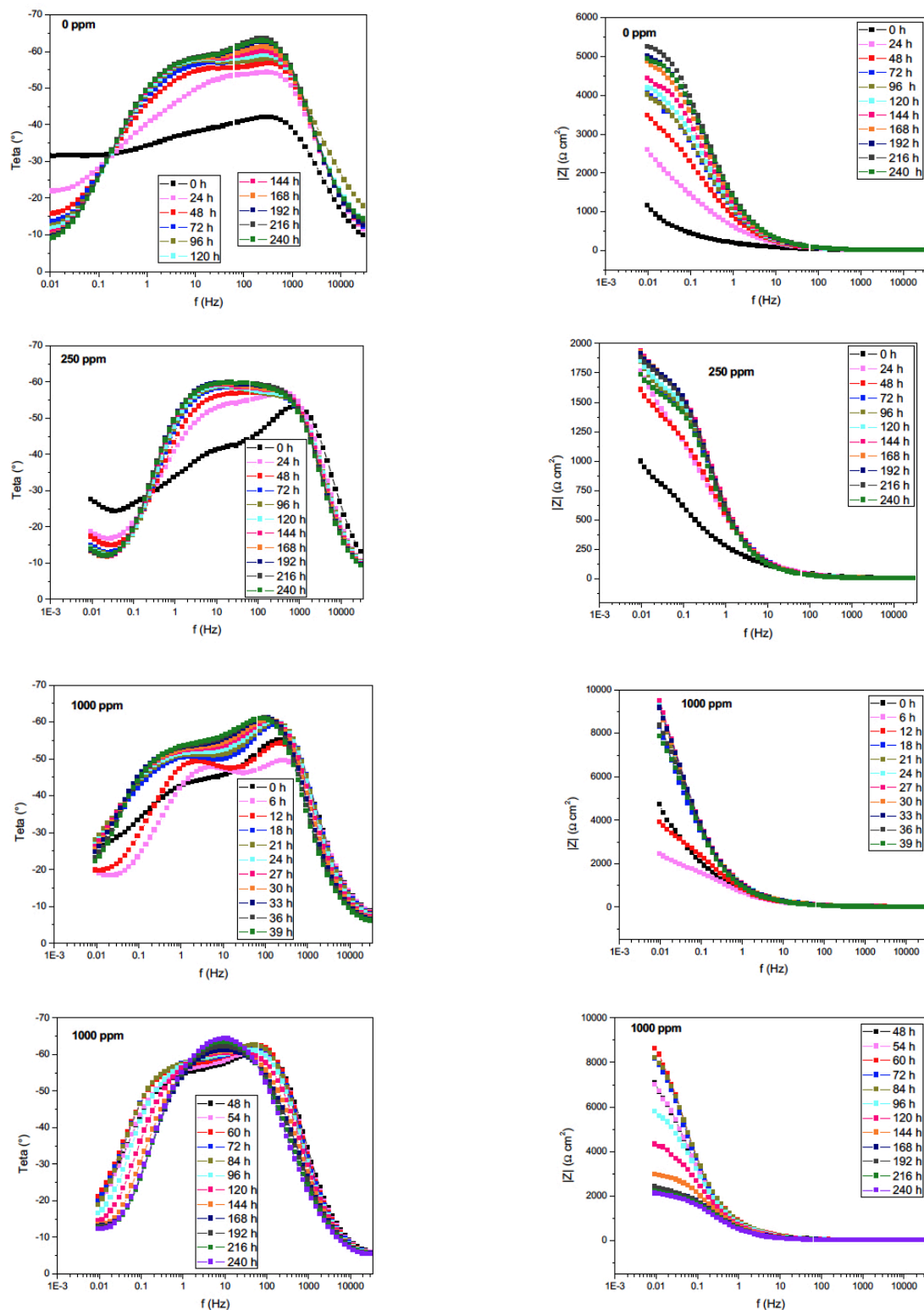


Fig. 3. Bode angle (left) and Bode modulus (right) diagrams of copper in synthetic seawater without and with GCI *E. arvensis*.

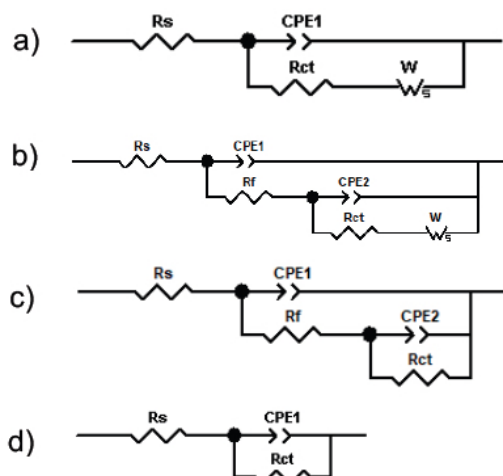


Fig. 4. Equivalent circuits proposed for copper in synthetic seawater without and with GCI *E. arvensis*.

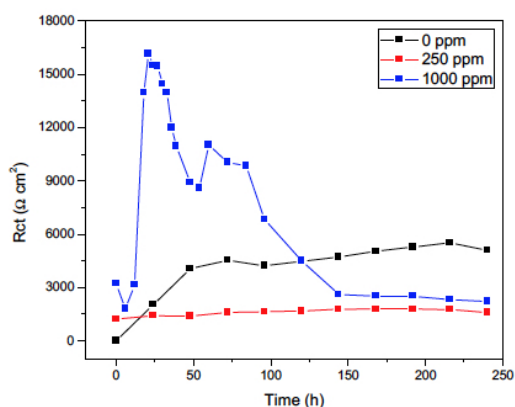


Fig. 5. Charge transfer resistance ( $R_{ct}$ ) of copper in synthetic seawater without and with GCI *E. arvensis*.

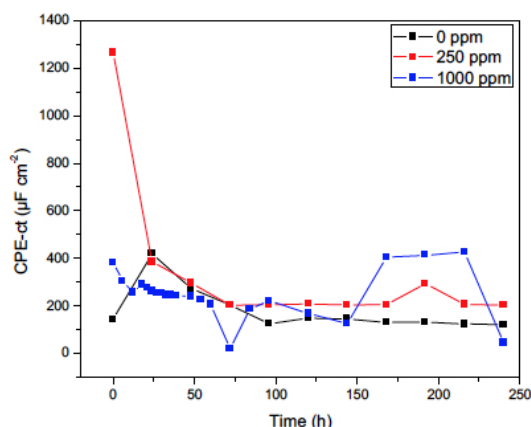


Fig. 6. Constant phase element of the charge transfer (CPE-ct) of copper in synthetic seawater without and with GCI *E. arvensis*.

The  $n$  values during the 240 h are close to 0.5 (0.5-0.7) for CPE-ct, suggesting that there is a mass transfer process. The  $n$  values for CPE-f are close to 1 (0.8), indicating that the corrosive system is more capacitive (Sherif and Park, 2006; Al-Mobarak *et al.*, 2010; Aperador *et al.*, 2012; Suarez *et al.*, 2013; Yu *et al.*, 2015). The corrosion IE % was determined using the Eq. (2) obtaining a maximum efficiency of 87.43% at 21 h.

### 3.3 Linear Polarization Resistance

The variation in the  $i_{corr}$  values for the copper exposed in synthetic seawater without and with GCI for ten days are shown in Fig. 7.  $i_{corr}$  values were determined from the  $R_p$  values and the Tafel slopes of the PPC. It can be observed that  $i_{corr}$  of the blank gradually decreased of 38.81 to 6.46  $\mu\text{A}/\text{cm}^2$ , which indicates the formation of corrosion products on the copper surface (Rihan *et al.*, 2014). In general, in presence of 250 ppm of the GCI, the  $i_{corr}$  shows a decrease along the exposure time. However, the corrosion current density values are higher than those obtained without GCI. At 1000 ppm, the  $i_{corr}$  increases during the first 9 h and then decreases until 96 h, leading to a lower corrosion rate. After this time, it can be observed another increase up 17.12  $\mu\text{A}/\text{cm}^2$  at the end of the exposure time. With the addition of 250 and 1000 ppm of GCI to the corrosive solution,  $i_{corr}$  at the end of the exposure was higher than that obtained in synthetic seawater without GCI.

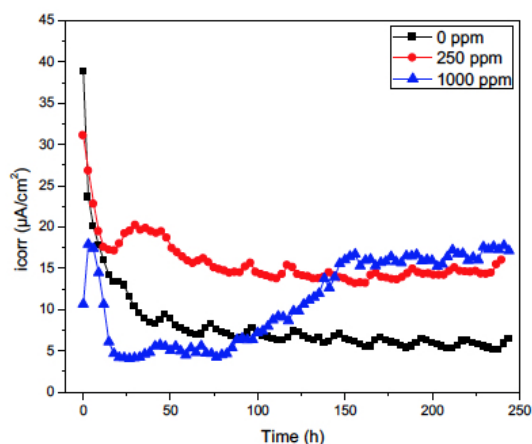


Fig. 7. Corrosion current density of copper exposed to synthetic seawater in absence and presence of two different concentrations of the GCI *E. arvensis* obtained from the LPR technique.



Accordingly to the results, the case with a concentration of 1000 ppm of GCI presented the lowest corrosion rate until the 87 h, afterwards,  $i_{corr}$  was increasing until the end of the exposure having the higher values of the three studied cases.

### 3.4 Scanning electron microscopy

The surface morphology of copper immersed in the synthetic seawater for ten days without and with GCI is observed from the images of Fig. 8. The image 8a shows the copper surface exposed in absence of the inhibitor, which presents corrosion products dispersed on the surface, whereas image 8b shows the surface free of corrosion products with some small pits. The scratches on the surface in all the images except the 8e were induced by the emery paper. Fig. 8c shows the surface of the copper exposed in the corrosive solution with 250 ppm of GCI, which presents more degradation than that exposed to the seawater with no GCI, revealing certain pitting corrosion once the surface was free of corrosion products (Fig.8d). With the addition of 1000 ppm of the GCI to the corrosive solution, it is possible to observe the formation of a film on the surface of the copper (Fig. 8e), however, the specimen without corrosion products showed the presence of corroded areas in localized form (Fig. 8f).

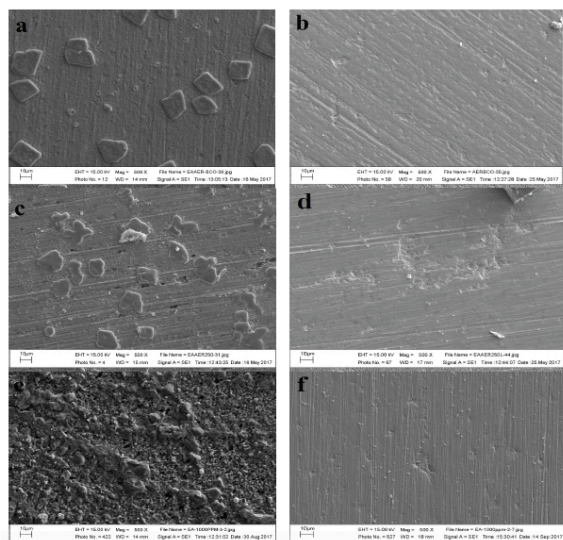


Fig. 8. SEM images of copper specimens exposed to synthetic seawater in absence of GCI (a, b), in presence of 250 ppm of GCI (c, d) and in presence of 1000 ppm of GCI (e, f), with corrosion products (left) and without corrosion products (right).

Table 3. EDS analysis of copper in synthetic seawater without and with GCI *E. arvense*.

Element	0 ppm	250 ppm	1000 ppm
	Composition (%)		
<b>Cu</b>	48.67	45.67	24.13
<b>Cl</b>	20.22	15.62	10.55
<b>O</b>	19.01	18.65	27.75
<b>Na</b>	6.58	3.15	—
<b>Mg</b>	3.57	2.5	3.76
<b>S</b>	1.2	—	—
<b>K</b>	0.75	0.64	2.19
<b>Ca</b>	—	2.38	—
<b>C</b>	—	11.39	31.6

SEM images after 10 days of immersion are in accordance with the results of EIS and RPL techniques, through which, it was demonstrated that the corrosion rate is higher than that of copper without GCI at the end of 240 h.

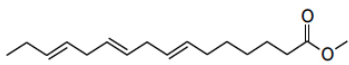
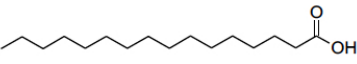
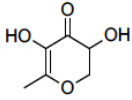
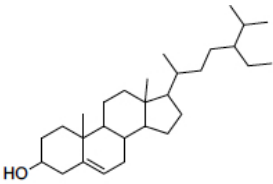
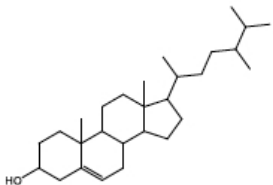
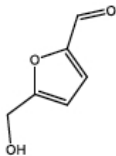
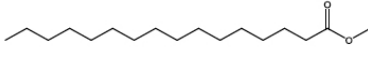
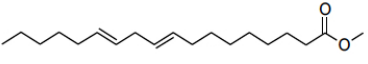
Table 3 shows the elemental chemical composition of the corrosion products of the copper exposed for 10 days in synthetic seawater without and with GCI. The elemental composition was obtained from the EDS analysis. It can be observed that the corrosion products of the copper exposed to the seawater without GCI present Cu, Cl and O in considerable concentrations, and Na, Mg, S and K in smaller concentrations.

At 250 ppm, in addition to the elements presented without GCI, the presence of C at a concentration of 11.39% was also identified. At 1000 ppm, it seems that the molecules of the GCI were partially adsorbed on the copper surface, finding the following composition in weight %: 31.6C, 24.13Cu, 10.55Cl and 27.75O, together with some small concentrations of Mg and K. The high concentration of carbon in the cases with GCI is probably due to the adsorption of the GCI over the metallic surface. The presence of oxygen may be due to both: the formation of CuO and the hydrolysis of the CuCl (Sherif and Park, 2006).

### 3.5 FTIR analysis

Fig. 9 shows the infrared spectrum of the GCI *E. arvense*. According to the spectrum, the following signals were found: around  $3347\text{ cm}^{-1}$  a wide signal characteristic of O-H (stretch), a signal at  $2922$  and  $2855\text{ cm}^{-1}$  (asymmetric stretching) is assignable to C-H type links. At  $1727\text{ cm}^{-1}$ , the C=O binding vibrations are shown, characteristics of the carbonyl group, and a signal at  $1050\text{ cm}^{-1}$  corresponding to the presence of C-O.

Table 4. Natural compounds present in GCI *Equisetum arvense*.

Compound	Abundance (%)	$t_r$ (min)	[M] <sup>+</sup>	Chemical structure
9,12,15-Octadecatrienoic acid, methyl ester (1)	18.63	21.1	292	
Hexadecanoic acid (2)	14.85	19.38	256	
2,3-dihydro-2,5-dihydroxy-6-methyl-4H-pyran-4one (3)	13.99	9.56	144	
Sitosterol (4)	9.68	37.03	414	
Campesterol (5)	6.29	32.25	400	
5-hydroxymethyl-2-furancarboxaldehyde (6)	4.79	10.74	126	
Hexadecanoic acid, methyl ester (7)	2.07	18.94	270	
9,12-octadecadienoic acid, methyl ester (8)	1.11	20.59	294	

$t_r$  = retention time from GC; [M<sup>+</sup>] molecular ion mass from MS

According to the literature, the presence of oxygen and double bonds in the chemical structures of the compounds used as corrosion inhibitors have proved to be good.

### 3.6 GC-MS analysis

In previous works, some vegetal species have been studied as natural corrosion inhibitors of metals

in seawater, which have not shown the chemical content of such species. So, the present work is the first research work trying to elucidate the chemical nature of the major compounds of the active extract as corrosion inhibitor in seawater. Analysis of the chemical content of the methanol extract of *E. arvense* was performed by gas chromatography coupled to mass spectrometry (GC-MS).

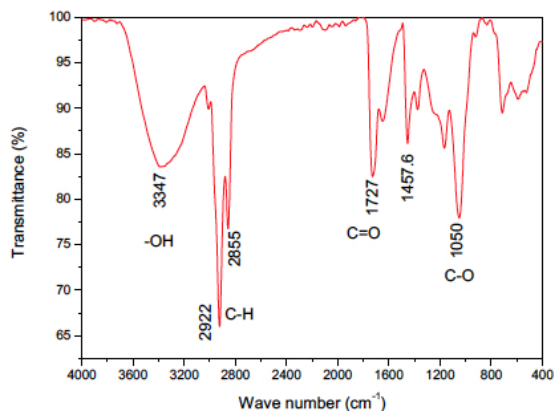


Fig. 9. Fourier transform-infrared spectroscopy of GCI *Equisetum arvense*.

Through this analytical technique the main chemical compounds of the *E. arvense* extract were identified through the next method: i) The compounds of the *E. arvense* extract taken into account from the gas chromatography analysis, were that whose signal presented the major area under the curve with respect to the total percentage of all the peaks; ii) according to the fragmentation pattern obtained through mass spectrometry analysis of the *E. arvense* extract, the identified compounds were that whose similarity was greater than 90% with respect to the standard compounds included in the equipment database. The identified compounds from CG-SM were compared to that reported in literature. Through this analysis, it was possible to identify eight components from the methanol extract of *E. arvense*. The identity, abundance and chemical structure of these compounds are shown in table 4. The results of the chemical composition of the methanol extract of *E. arvense* is the next: an aromatic ketone (3) 13%, fatty acids and their respective esters (1, 2, 7, 8) about 36%; an aldehyde (6) in more than 4%, terpenes (4 and 5) in 15%. Fatty acids have been found in natural inhibitors studied as reducers of the corrosion rate of metals in acid media. Eddy *et al.* (2012) reported that the Daniella oliverri gum exudate inhibited a 72% of the corrosion presented in mild steel exposed to hydrochloric acid 0.1 M, when 500 mg/L of the gum was used, mentioning that this inhibitor contains a 16.59% of hexadecanoic acid. The 2,3-dihydro-2,5-dihydroxy-6-methyl-4H-pyran-4-one (aromatic ketone) also known as dihydrohydroxy maltol is an unusual sugar that was reported by Yoshiki and Okubo (1995) after being isolated from hypocotyls of soybean. This compound shows no history of being studied as a corrosion inhibitor.

Regarding to the other compounds present in *E. arvense*, they are not reported as corrosion inhibitors. From the chemical results above mentioned, it is possible to distinguish that the inhibitory activity reported in this work for *E. arvense* as corrosion inhibitor was derived from the set of compounds present in the methanol extract of this plant species.

## Conclusions

According to the PPC, the GCI is classified as a mixed-type inhibitor; which can be adsorbed onto the metal surface by blocking the active copper sites. The results of EIS showed that the dominant process in the corrosion inhibition by the GCI occurs through a mass transfer process. The corrosion current density ( $i_{corr}$ ) had an oscillatory behavior with slight tendency to decrease for that cases without and with GCI, as evidence of the continuous dissolution/recovery of the corrosion products layer and/or adsorption of the GCI onto the surface of the copper. In the case of 1000 ppm, the  $i_{corr}$  is smaller than that of the blank until 87 h. The effectiveness of the GCI to this concentration is attributed to the adsorption of the GCI on the metal surface, which was corroborated with the SEM results. From the FTIR technique, it was determined that the GCI mainly contains compounds whose chemical structure has functional groups such as -OH, C=O, C-O and bonds C-H. Through GC-MS, it was possible to identify eight main compounds, including a ketone, fatty acids and their respective esters, as well as an aldehyde and two terpenes. These compounds must be the responsible for the layer formed on the surface of the copper to retard the corrosion process in the synthetic seawater.

## Acknowledgements

The student Ana Esquivel R. thanks to The National Council of Science and Technology (CONACYT) for the scholarship granted to study the PhD in engineering and applied sciences program of the Engineering and Applied Sciences Research Centre at the Autonomous University of Morelos State with the scholarship number 305336. The authors grateful to the National Laboratory of Analytical Chemistry of the Chemical Researches Center (CIQ) of the Autonomous University of Morelos State, for the facilities granted in the technical assistance for the analysis of GC-MS.

## Nomenclature

CPE	Constant phase element
$E_{corr}$	Corrosion potencial
EDS	Energy dispersive X-Ray spectroscopy
EIS	Electrochemical impedance spectroscopy
FTIR	Fourier transform-infrared spectroscopy
GCI	Green corrosión inhibitor
GC-MS	Gas chromatography coupled to mass spectroscopy
GDP	Gross domestic product
h	Hours
$i_{corr}$	Corrosion current
IE	Inhibition efficiency
L	Liters
LPR	Linear polarization resistance
mA	Milliamps
mg	Milligrams
mV	Millivolts
n	Constant related to the scattering angle
PPC	Potentiodynamic polarization curves
ppm	Parts per million
$R_{ct}$	Charge transfer resistance
$R_f$	Film resistance
$R_p$	Polarization resistance
$R_s$	Solution resistance
SEM	Scanning electron microscopy
$T_f$	Final time
$T_i$	Initial time
W	Warburg impedance
<i>Greek symbols</i>	
$\beta_a$	Anodic slope
$\mu A$	micro-amps
$\Omega$	Ohm

## References

- Abdallah, M., Radwan, M., Shahera, Shohayeb, S. and Abdelhamed, S. (2010). Use of some natural oils as crude pipeline corrosion inhibitors in sodium hydroxide solutions. *Chemistry and Technology of Fuels and Oils* 46, 354-362.
- Abdullah, M. D. (2011). A review: plant extracts and oils as corrosion inhibitors in aggressive media. *Industrial Lubrication and Tribology* 63, 227-233.
- Al-Mhyawi, S. R. (2014). Inhibition of steel corrosion in natural seawater using natural inhibitor (Algae). *Asian Journal of Chemistry* 26, 7804-7810.
- Al-Mobarak, N. A., Khaled, K. F., Hamed, M. N. H., Abdel-Azim, K. M. and Abdelshafi, N. S. (2010). Corrosion inhibition of copper in chloride media by 2-mercapto-4-(p-methoxyphenyl)-6-oxo-1,6-dihydropyrimidine-5-carbonitrile: Electrochemical and theoretical study. *Arabian Journal of Chemistry* 3, 233-242.
- Al-Otaibi, M., Al-Mayouf, A., Khan, M., Mousa, A., Al-Mazroa, S. and Alkathlan, H. (2014). Corrosion inhibitory action of some plant extracts on the corrosion of mild steel in acidic media. *Arabian Journal of Chemistry* 7, 340-346.
- Al-Snafi, A. E. (2017). The pharmacology of *Equisetum arvense* - A review. *IOSR Journal of Pharmacy* 7, 31-42.
- Anupama, K.K., Ramya, K., Shainy, K. M. and Joseph, A. (2015). Adsorption and electrochemical studies of *Pimenta dioica* leaf extracts as corrosion inhibitor for mild steel in hydrochloric acid. *Materials Chemistry and Physics* 167, 28-41.
- Aperador, W., Bautista, R. J. H. and Pardo, C. O. (2012). Electrochemical behavior of thin films of CrN/Cr obtained varying the bias potential. *Revista Mexicana de Ingeniería Química* 11, 145-154.
- Asgarpanah, J. and Roohi, E. (2012). Phytochemistry and pharmacological properties of *Equisetum arvense* L. *Journal of Medicinal Plants Research* 6, 3689-3693.
- ASTM D 1141 - 98. (2003). *Standard Practice for the Preparation of Substitute Ocean Water*.
- Banerjee, S., Srivastava, V. and Singh, M. M. (2012). Chemically modified natural polysaccharide as green corrosion inhibitor for mild steel in acidic medium. *Corrosion Science* 59, 35-41.
- Brunoro, G., Frignani, A., Colledan, A. and Chiavari, C. (2003). Organic films for protection of copper and bronze against acid rain corrosion. *Corrosion Science* 45, 2219-2231.

- Callister, W.D. Jr. and Rethwisch, D. G. (2009) *Materials Science and Engineering an Introduction*. 8th Edition. Edited by John Wiley & Sons Inc., New Jersey.
- Chen, W., Hong, S., Li, H. B., Luo, H. Q., Li, M. and Li, N. B. (2012). Protection of copper corrosion in 0.5M NaCl solution by modification of 5-mercapto-3-phenyl-1,3,4-thiadiazole-2-thione potassium self-assembled monolayer. *Corrosion Science* 61, 53-62.
- Deyab, M. A., Essehlib, R. and El Bali, B. (2015). Inhibition of copper corrosion in cooling seawater under flowing conditions by novel pyrophosphate. *The Royal Society of Chemistry* 5, 64326-64334.
- Eddy, N. O., Odiongenyi, A. O., Ameh, P. O. and Ebenso, E. E. (2012). Corrosion inhibition potential of Daniella oliverri gum exudate for mild steel in acidic medium. *International Journal of Electrochemical Science* 7, 7425 - 7439.
- El-Etre, A. Y. (1998). Natural honey as corrosion inhibitor for metals and alloys [I] copper in neutral aqueous solution. *Corrosion Science* 40, 1845-50.
- Fares, M. M., Maayta, A. K. and Al-Qudah, M. M. (2012). Pectin as promising green corrosion inhibitor of aluminum in hydrochloric acid solution. *Corrosion Science* 60, 112-117.
- Feng, L., Yang, H. and Wang, F. (2011). Experimental and theoretical studies for corrosion inhibition of carbon steel by imidazoline derivative in 5% NaCl saturated Ca(OH)<sub>2</sub> solution. *Electrochimica Acta* 58, 427-436.
- Flores-De los Ríos, J. P., Sánchez-Carrillo, M., Nava-Din, C. G., Chacón-Nava, J. G., Escobedo-Bretado, M. A., Monreal-Romero, H. A., Bautista-Margulis, R. G., Neri-Flores, M. A. and Martínez-Villafañe, A. (2015). Corrosion inhibition of mild steel using Agavoideae extract in 1M HCl solution. *International Journal of Electrochemical Science* 10, 10210-10222.
- Gopi, D., Govindaraju, K.M., Collins, A. P. V., Angeline, D. M. and Kavitha, L. (2009). A study on new benzotriazole derivatives as inhibitors on copper corrosion in ground water. *Corrosion Science* 51, 2259-2265.
- Hong, S., Chen, W., Qun, L. H. and Bing, L. N. (2012). Inhibition effect of 4-amino antipyrine on the corrosion of copper in 3 wt % NaCl solution. *Corrosion Science* 57, 270-278.
- Hu, L., Zhang, S., Li, W. and Hou, B. (2010). Electrochemical and thermodynamic investigation of diniconazole and triadimefon as corrosion inhibitors for copper in synthetic seawater. *Corrosion Science* 52, 2891-2896.
- Koch, G. H., Brongers, M. P. H., Thompson, N. G., Virmani, Y. P. and Payer, J. H. (2002). Corrosion costs and preventive strategies in the United States. *NACE No. FHWA-RD-01-156*.
- Li, L., Zhang, X., Lei, J., He, J., Zhang, S. and Pan, F. (2012). Adsorption and corrosion inhibition of *Osmanthus fragran* leaves extract on carbon steel. *Corrosion Science* 63, 82-90.
- Motawea, M. M., El-Hossiany, A. and Fouda, A. S. (2019). Corrosion control of copper in nitric acid solution using *Chenopodium* extract. *International Journal of Electrochemistry Science* 14, 1372-87.
- Oguzie, E. E. (2008). Evaluation of the inhibitive effect of some plant extracts on the acid corrosion of mild Steel. *Corrosion Science* 50, 2993-2998.
- Oniszcuka, A., Podgórska, R., Oniszcukb, T., Zukiewicz-Sobczakc, W., Nowakd, R. and Waksmundzka-Hajnos, M. (2014). Extraction methods for the determination of phenolic compounds from *Equisetum arvense* L. herb. *Industrial Crops and Products* 6, 377-381.
- Oukhrib, R., El Issami, S., Chaouay, A., El Mouaden, K., Jmiai, A., El Ibrahim, B., Bazzi, L., Bammou, L. and Hilali, M. (2015). The inhibitory effect of saffron extract (*Crocus sativus* L) on copper corrosion in seawater. *Chemical Science Review and Letters* 4, 241-251.
- Oukhrib, R., El Issami, El Ibrahim B., El Mouaden K., Bazzi L., Bammou L., Chaouay, A., Salghi, R., Jodeh, S., Hammouti, B. and Amin-Alami, A. (2017). Ziziphus lotus as green inhibitor of Copper corrosion in natural sea water. *Portugaliae Electrochimica Acta* 35, 187-200.

- Pallag, A., Filip, G. A., Olteanu, D., Clichici, S., Baldea, I., Jurca, T., Micle, O., Vicaș, L., Marian, E., Sorișău, O., Cenariu, M. and Mureșan, M. (2018). *Equisetum arvense* L. extract induces antibacterial activity and modulates oxidative stress, inflammation, and apoptosis in endothelial vascular cells exposed to hyperosmotic stress. *Oxidative Medicine and Cellular Longevity* 2018, 1-14.
- Pallag, A., Jurca, T., Pasca, B., Sirbu, V., Honiges, A. and Costuleanu, M. (2016). Analysis of phenolic compounds composition by HPLC and assessment of antioxidant capacity in *Equisetum arvense* L. extracts. *Revista de Chimie (Bucharest)* 67, 1623-1627
- Rahal, C., Masmoudi, M., Abdelhedi, R., Sabot, R., Jeannin, M., Bouaziz, M. and Refait P. (2016). Olive leaf extract as natural corrosion inhibitor for pure Copper in 0.5 M NaCl solution: a study by voltammetry around OCP. *Journal of Electroanalytical Chemistry* 769, 53-61.
- Raichev, R., Veleva, L. and Valdez, B. (2009). *Corrosión de metales y degradación de materiales*. CINVESTAV-MÉRIDA/UABC-MEXICALI.
- Raj, X. J. and Nallaiyan, R. (2012). Corrosion inhibitive properties and electrochemical adsorption behavior of some piperidine derivatives on brass in natural sea water. *Journal of Solid State Electrochemistry* 16, 391-402.
- Rani, D. P. and Selvaraj, S. (2010). Emblica officinalis (AMLA) leaves extract as corrosion inhibitor for Copper and its alloy (CU-27ZN) in natural sea water. *Archives of Applied Science Research* 2, 140-150.
- Rihan, R., Shawabkeh, R. and Al-Bakr, N. (2014). The effect of two amine-based corrosion inhibitors in improving the corrosion resistance of carbon steel in sea water. *Journal of Materials Engineering and Performance* 23, 693-699.
- Sastri, V. S. (2011). Adsorption in corrosion inhibition. In: *Green Corrosion Inhibitors. Theory and Practice*. (Winston Revie Ed.), Pp. 103-138. John Wiley & Sons Inc., New Jersey.
- Sherif, E. M. and Park, S. M. (2006). 2-amino-5-ethyl-1, 3, 4- thiadiazole as a corrosion inhibitor for copper in 3.0% NaCl solutions. *Corrosion Science* 48, 4065-4079.
- Shylesha, B. S., Venkatesha, T. V. and Praveen, B. M. (2011). Corrosion inhibition studies of mild steel by new inhibitor in different corrosive medium. *Research Journal of Chemical Sciences* 1, 46-50.
- Singh, A. K., Mohapatra, S. and Pani, B. (2016). Corrosion inhibition effect of Aloe vera gel: Gravimetric and electrochemical study. *Journal of Industrial and Engineering Chemistry* 33, 288-297.
- Suarez, O. J., Olaya, J. J. and Rodil, S. (2013). The effect of operating conditions during plating on the electrochemical behavior and morphology of trivalent solution-derived chromium coatings. *Revista Mexicana de Ingeniería Química* 12, 129-141.
- Tian, H., Li, W. and Hou, B. (2011). Novel application of a hormone biosynthetic inhibitor for the corrosion resistance enhancement of copper in synthetic seawater. *Corrosion Science* 53, 3435-3445.
- Yoshiki, Y. and Okubo, K. (1995). Active oxygen scavenging activity of DDMP (2,3-dihydro-2,5-dihydroxy-6-methyl-4H-pyran-4-one) saponin in soybean seed. *Bioscience, Biotechnology and Biochemistry* 59, 1556-1557.
- Yu, Y., Zhang, D., Zeng, H., Xie, B., Gao, L. and Lin, T. (2015). Synergistic effects of sodium lauroyl sarcosinate and glutamic acid in inhibition assembly against copper corrosion in acidic solution. *Applied Surface Science* 355, 1229-1237.